

Closed Loop Optimization of Opto-Mechanical Structure via Mechanical and Optical analysis software

David Bonin, Opto-Mechanical Engineer
Brian McMaster, Senior Opto-Mechanical Engineer
Corning Tropel Corporation, Fairport, New York

Abstract:

This paper will discuss how mechanical and optical analysis software can be used together to optimize an opto-mechanical structure subjected to vibrational loading. Mechanical analysis software output is post processed into Zernike polynomial coefficients and rigid body motions for analysis with optical modeling software. Structural modifications can then be implemented to improve optical performance.

A Cassegrain telescope, which can be utilized for laser radar applications, will be used to demonstrate this optimization. Two FEA solution methods are compared. Based on the deformation results of the FEA, Zernike polynomials and rigid body motions are generated and applied to the optical surfaces in CODE V®. The effect of these deformations on wavefront can then be computed and compared to a required performance.

1. INTRODUCTION

The manufacturing and testing of prototypes to verify designs is usually expensive and not practical from a scheduling standpoint. Having the ability to analyze an opto-mechanical structure and predict the change in wavefront caused by vibrational loading allows optimization of the structure without the costly production of prototypes.

In this example, a Cassegrain telescope (Figures 1 & 2) subjected to a random vibration in a single direction will be analyzed. The Cassegrain telescope consists of three parts; the primary mirror, the secondary mirror and the mechanical structure connecting the two mirrors which is called the spider. The random vibration is specified by a given PSD (Power Spectral Density) function. Two different methods will be used to analyze the secondary mirror of the telescope, one static and one dynamic, and the results from the two analyses will be compared. Both methods will utilize NX Nastran to perform a Finite Element Analysis on the telescope. The surface deformations from the FEA will then be converted to Zernike coefficients using SIGFIT, a commercially available software package. The Zernike coefficients can then be applied to the optical surfaces in CODE V® to evaluate the affect of the disturbance on wavefront.

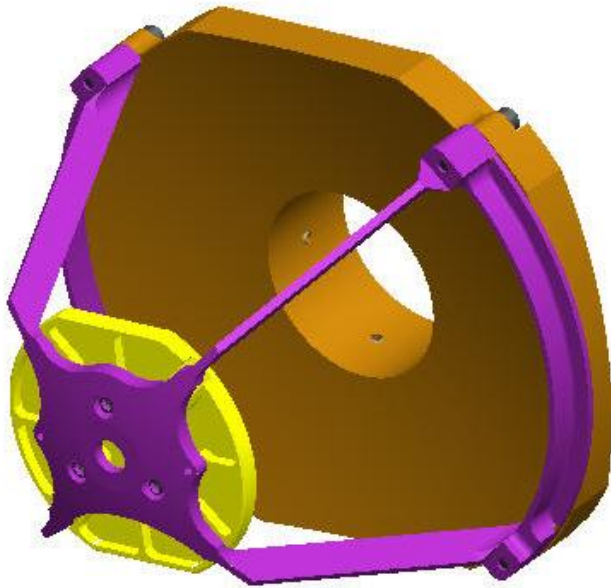
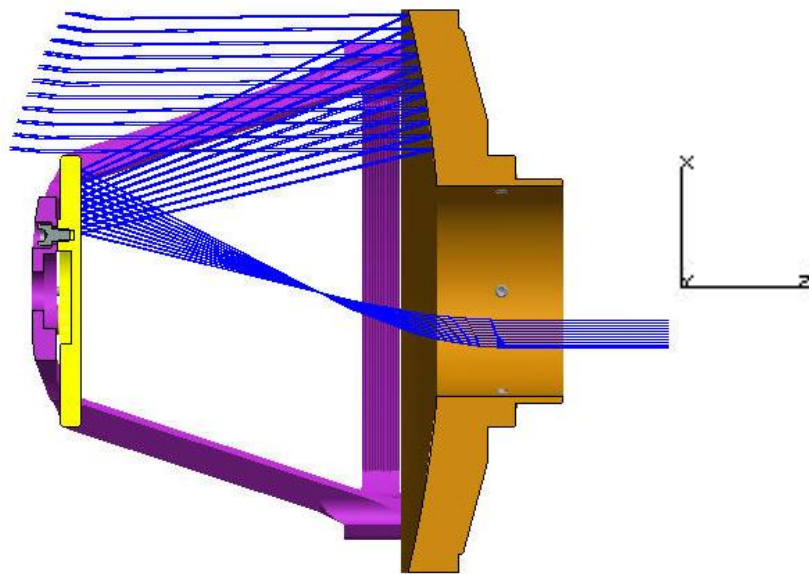


Figure 1: Isometric view of Cassegrain Telescope

Figure 2: Cross-section view of Cassegrain Telescope showing optical ray trace



2. THE FINITE ELEMENT MODEL (Figures 3 & 4)

The finite element model is made up of a combination of parabolic tetrahedron elements and brick elements. Each mirror surface is covered with a layer of 2D elements (orange) primarily for nodal bookkeeping. The bolted interfaces were approximated with 2X bolt diameter connectivity. The structure is restrained at three points on the backside of the primary mirror which are connected by rigid elements to a single node. For the static analysis this node is fixed in all six degrees of freedom. For the dynamic analysis this node represents the vibration source and is fixed in all degrees of freedom except one oriented in the radial direction (X).

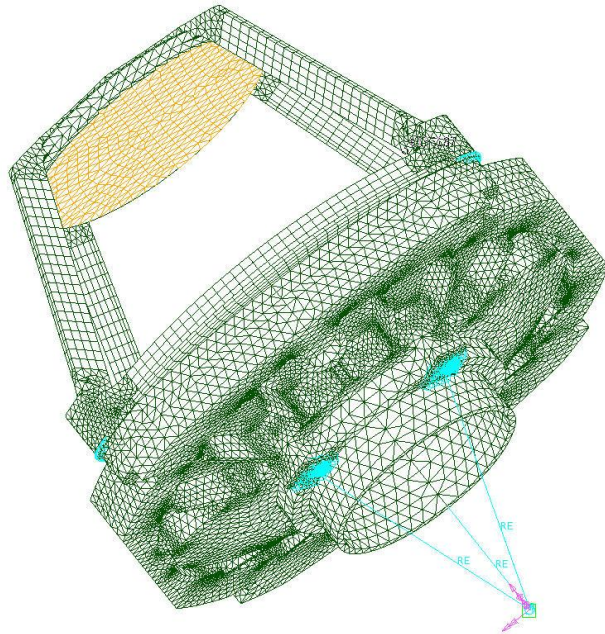


Figure 3

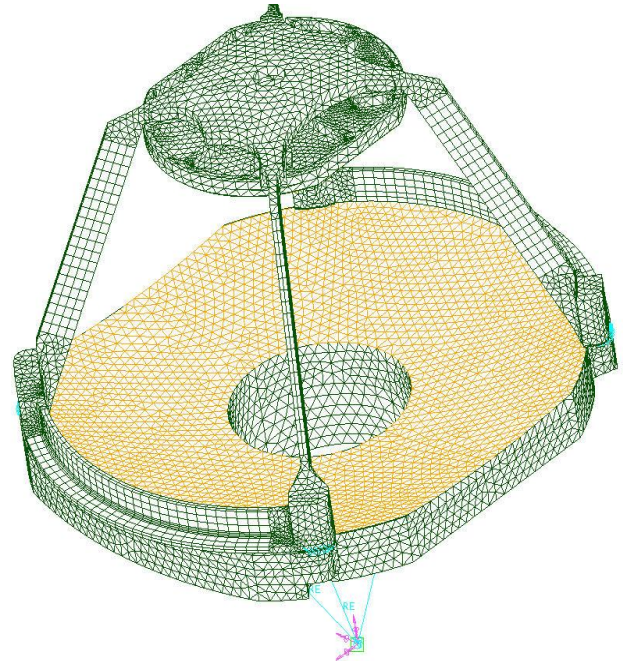


Figure 4

3. STATIC ANALYSIS

In order to solve a random vibration problem using static analysis the equivalent G-load response must be calculated. This requires several assumptions: a single degree of freedom system, a random acceleration whose spectrum is flat in the area of resonance and lightly damped.

With these assumptions the following equation will be used to determine the equivalent static G-load [1].

$$G := \sqrt{\frac{\pi}{2} \cdot \text{PSD}_n \cdot f_n \cdot Q}$$

PSD = G^2/Hz input at resonance frequency

f = resonance frequency

Q = transmissibility

A FEA model was used to determine the first three resonant frequencies.

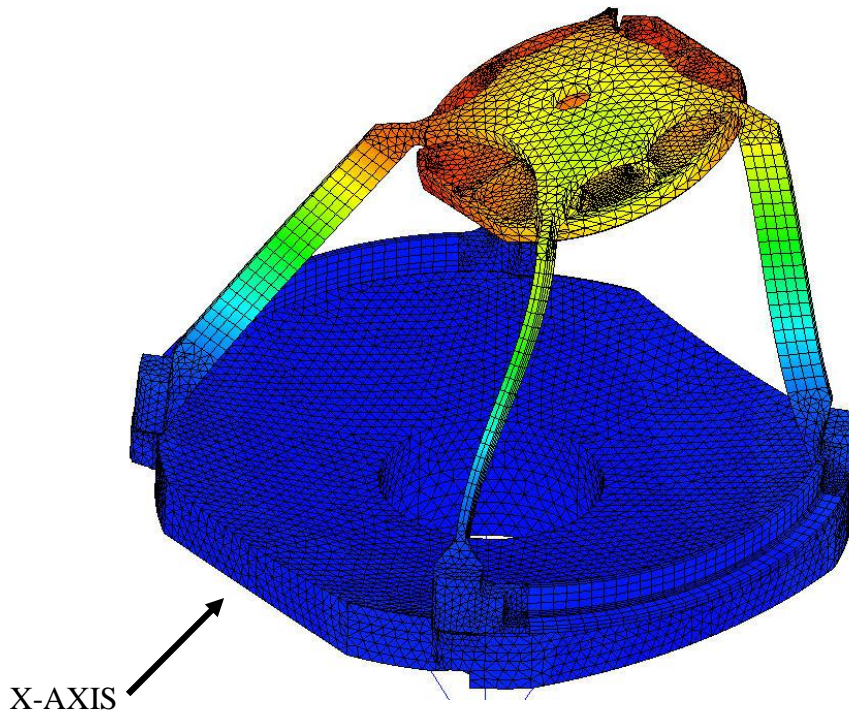


Figure 5
MODE 1
468 Hz

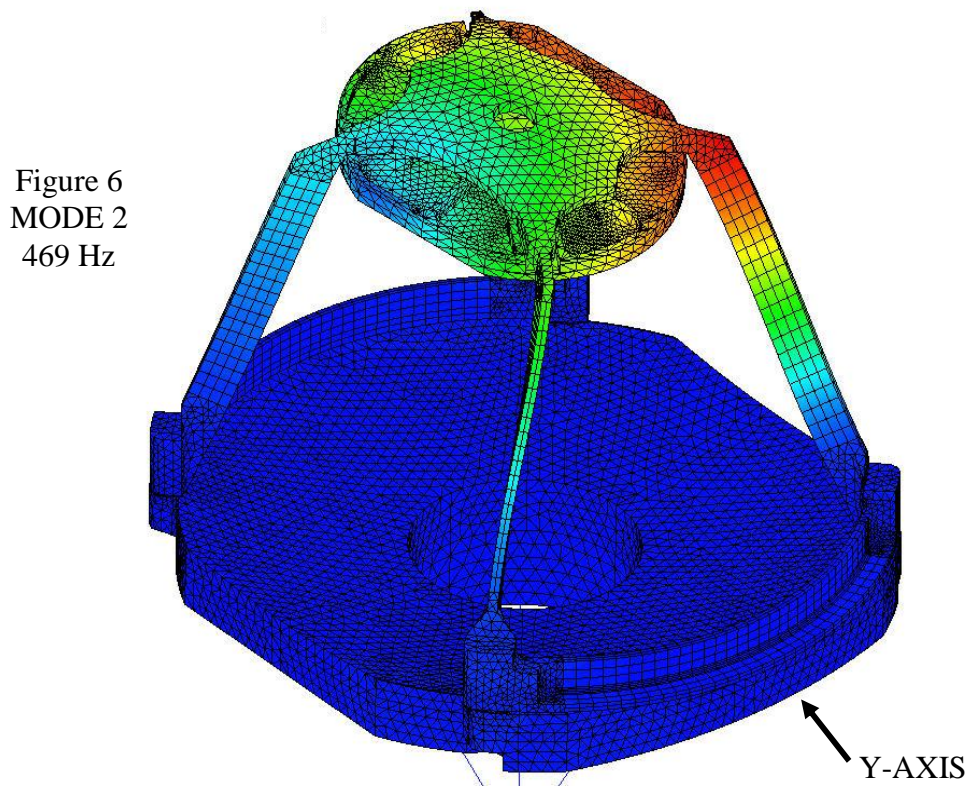


Figure 6
MODE 2
469 Hz

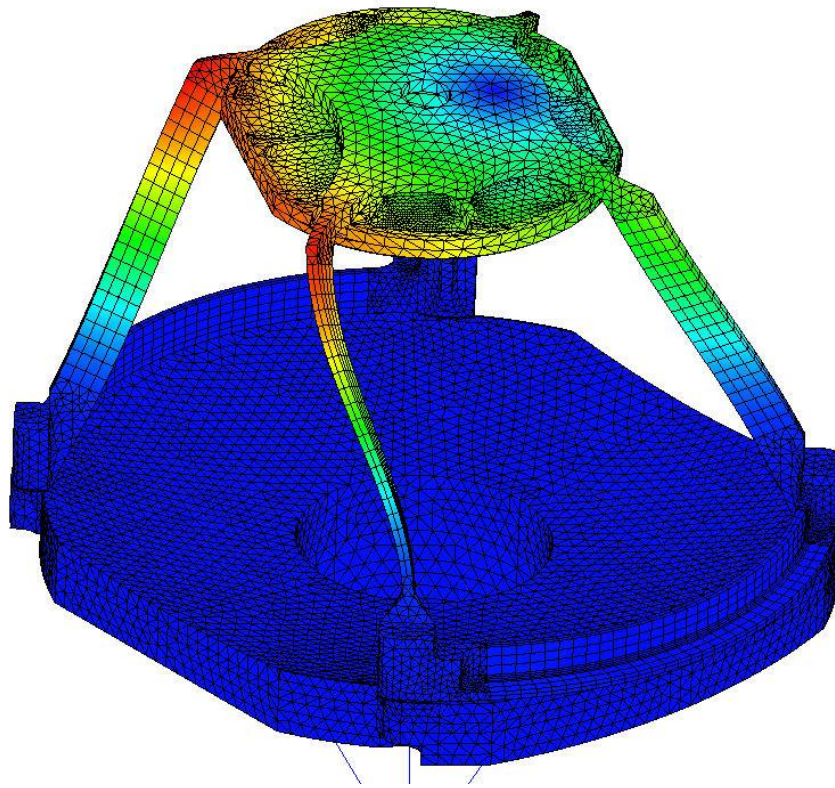


Figure 7
MODE 3
476 Hz

These three modes have very distinct mode shapes and are separated by less than 10 Hz. For a worst case example, mode 1 is used with the X-direction forcing function because mode 1 is predominately X displacement.

Using the mode 1 resonance frequency value (468 Hz) and the given PSD function (Figure 8) it is determined that the PSD value is .0025 G^2/Hz .

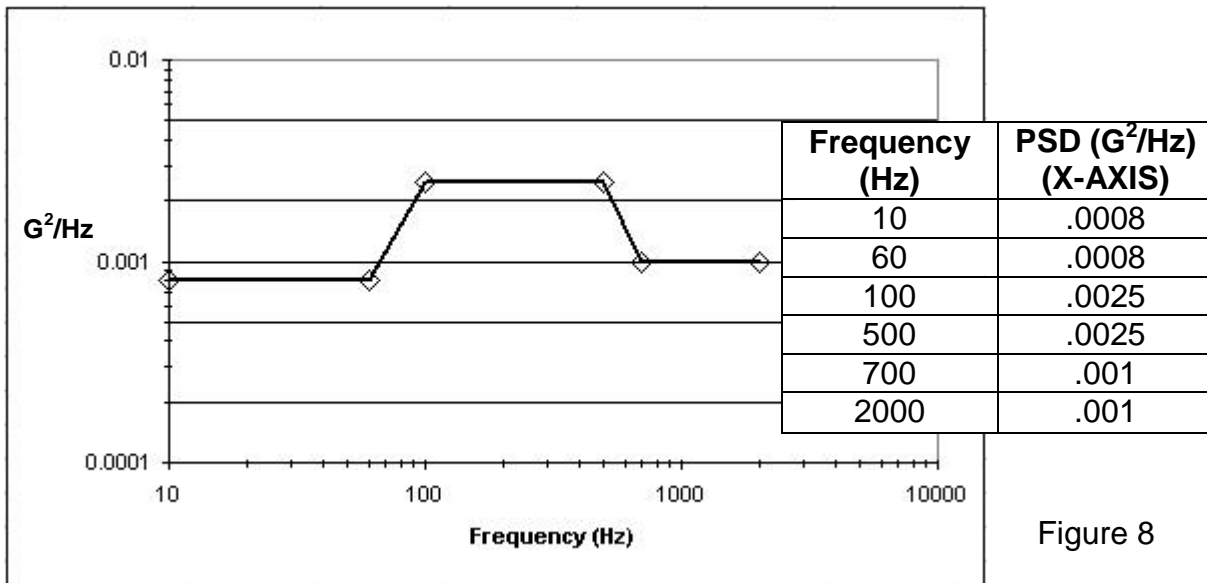


Figure 8

The transmissibility (Q) of a lightly damped “beam-type” structure is approximated by substituting the resonant frequency into the following expression [1]:

$$Q = 2(\omega_n)^{1/2} = 43.27$$

Now the equation for the equivalent G-load can be evaluated using the values for PSD, resonant frequency, and transmissibility resulting in a value of 8.9 G's.

This G-load was then applied to a static FEA with the load applied in the X-direction. Figure 9 shows the results of that analysis.

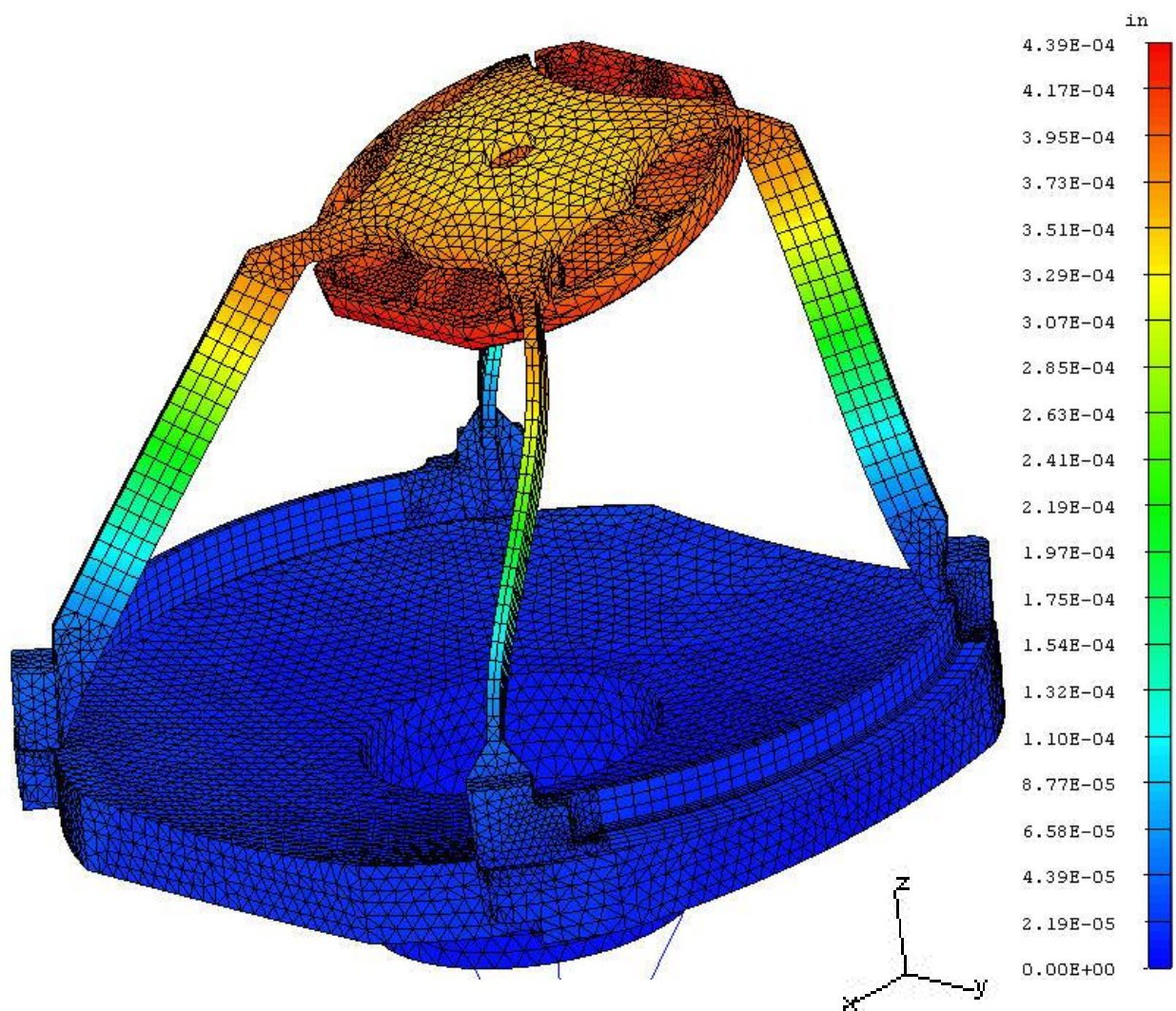


Figure 9

Using the nodal displacement data from the surfaces, SIGFIT performs a fitting analysis to represent the shape of the surface with Zernike coefficients and rigid body motions. The Zernikes generated for the secondary mirror are shown in Table 1.

```

! Loadcase= 1   FEA Case ID= 1   Surface Sign= 1
! Optic # = 1   OpticLabel=secondary
! Frn-Zer Polynomial Coefficients
! INR S01  2.5028E+01
S01 L01
ZFR 37 SUR SSZ 1.0 WVL  6.32790E-01
-2.65615E-04 -2.58857E-05 -3.80010E-07 -2.45874E-03 -7.17180E-03 -3.66432E-03
-7.78828E-04  2.12265E-03  4.28425E-04  1.32968E-04  4.74682E-04  1.87110E-03
 2.21708E-03  1.09550E-03 -1.31573E-03 -1.87863E-04  1.26491E-03 -4.90716E-04
-3.18804E-04  2.22943E-04 -1.44735E-03 -1.59834E-03 -7.29451E-04  7.09694E-04
 5.80135E-06 -1.68636E-04  9.75339E-05 -7.10719E-04  4.59032E-04  2.34152E-04
-1.29017E-04  6.48591E-04  9.74422E-04  0.00000E+00  0.00000E+00  1.47499E-04
 0.00000E+00

```

Table 1-Static Analysis Zernike Coefficients

These Zernikes will be compared to the random analysis results to evaluate the validity of the static analysis assumptions.

4. RANDOM ANALYSIS

As in the static analysis, this example will only examine the X-direction. The first step to the random analysis is to generate mode shapes. This modal analysis is similar to the one performed for the static analysis with slightly modified boundary conditions. A large mass is added to the vibration source node. To allow vibration in the X-direction, this node is unconstrained in X. The results of the modal analysis are the same as the previous static analysis results with a rigid body mode included.

Using the modal shape data for the secondary mirror surface, the PSD table (Figure 8), and assuming a damping value of 1 percent, a random analysis is performed. The output from this first random analysis is a modal contribution table.

The modal contributions for the secondary mirror are shown in table 2. They include percentage contribution for rigid body motion (RB), for Power (d-RoC), and for surface RMS (S-RMS) with the given PSD. Nearly 90% of the surface RMS comes from the first mode justifying the decision to excite in the X-direction to get worst case.

```

Each modes % contribution to PSD for Surface= 1
Mode      Freq  RB-Tx  RB-Ty  RB-Tz  RB-Rx  RB-Ry  d-RoC  d-CoC  S-RMS  R-RMS
 1      467.88 99.298 56.275 43.004 56.574 99.302 99.959 99.959 89.098 73.983
 2      468.79  0.700 42.969 55.627 42.677  0.696  0.000  0.000 10.737 75.306
 3      475.50  0.002  0.756  1.369  0.749  0.002  0.041  0.041  0.164  0.711

```

Table 2-Modal Contribution Table

Because both the rigid body motion and surface RMS are dominated by the contribution from Mode 2, A fitting analysis is performed on this mode to represent the shape of the secondary mirror surface deformation. This is similar to the analysis performed for the static solution and results in the following Zernike coefficients (Table 3).

```

! Loadcase= 1   FEA Case ID= 2   Surface Sign= 1
! Optic # = 1   OpticLabel=secondary
! Frn-Zer Polynomial Coefficients
! INR S01  2.5028E+01
S01 L01
ZFR 37 SUR SSZ 1.0 WVLS  6.32790E-01
 9.84836E+01  1.14089E+02  6.16968E+00  4.11998E+01  3.23545E+03 -9.41415E+02
 2.11677E+03  6.32480E+02 -3.25373E+01 -6.87915E+02  2.63856E+02 -6.57182E+02
 5.41013E+01 -9.23953E+02 -2.26712E+02  1.38631E+01  1.47095E+02  6.48928E+01
 1.22111E+02 -1.11918E+02  2.54792E+02  3.84360E+01  2.58017E+02  3.79771E+01
-2.69338E+01  2.18908E+01  3.72518E+01 -1.72783E+02 -6.07544E+01 -6.42724E+01
 6.67980E+01 -1.08266E+02 -5.40337E+01  0.00000E+00  0.00000E+00 -1.91192E+01
 0.00000E+00

```

Table 3-Random Analysis Mode 1 Zernike Coefficients

This analysis provides the shape function of the deformed surface with rigid body motions removed. It should be noted that these are normalized values. A surface RMS, based on these normalized values, is calculated and will be used to properly scale these Zernikes.

A second random analysis is performed using only mode 1 data to determine the actual surface RMS contribution from mode 1. This value is for a one sigma condition (values will not be exceeded 68% of the time).

These two surface RMS values can be used to calculate a scaling factor.

$$\text{Scaling Factor} = \frac{\text{surface RMS}_{\text{mode 1 random}}}{\text{surface RMS}_{\text{mode 1 fitting}}}$$

The random analysis mode 1 rigid body motions and Zernike coefficients are scaled with this scaling factor to provide actual surface deformations due to mode 1 when the model is excited in the X-direction for one sigma values.

The wavefront aberrations created by the surface irregularities and rigid body motions can then be evaluated against specification. At this point a decision can be made whether the structure is adequate or requires improvement.

5. STATIC AND DYNAMIC SOLUTIONS COMPARISON

Because the random analysis deformations were so dominated by contributions from mode 1, it was expected that there would be some correlation between the shape functions generated by the two different analyses. The magnitude of the surface RMS and rigid body motions were expected to vary since the assumptions made to calculate the equivalent static g-load “loosely” fit the criteria for the assumptions required. However, a comparison of the shape functions generated by the two analysis methods shows very little correlation (see table 5). Further investigation is required to understand the differences in the two analyses.

Therefore, the more rigorous random analysis results will be used to validate optical performance.

ZERN	RANDOM	STATIC	RATIO	ZERN	RANDOM	STATIC	RATIO	ZERN	RANDOM	STATIC	RATIO	ZERN	RANDOM	STATIC	RATIO
1	1.00E+00	1.00E+00	1.00	11	1.02E-02	-3.76E+03	-2.70E-06	21	1.12E-01	-3.82E+01	-2.92E-03	31	2.13E-01	-4.21E+02	-5.07E-04
2	1.16E+00	9.75E-02	11.89	12	2.03E-02	-4.36E+03	-4.66E-06	22	1.22E-01	-7.65E+01	-1.59E-03	32	2.23E-01	-4.59E+02	-4.87E-04
3	6.26E-02	1.43E-03	43.79	13	3.05E-02	-2.36E+02	-1.29E-04	23	1.32E-01	-1.15E+02	-1.15E-03	33	2.34E-01	-4.97E+02	-4.70E-04
4	4.18E-01	9.26E+00	0.05	14	4.06E-02	-1.57E+03	-2.58E-05	24	1.42E-01	-1.53E+02	-9.30E-04	34	2.44E-01	-5.35E+02	-4.55E-04
5	3.29E+01	2.70E+01	1.22	15	5.08E-02	-1.24E+05	-4.10E-07	25	1.52E-01	-1.91E+02	-7.97E-04	35	2.54E-01	-5.73E+02	-4.43E-04
6	-9.56E+00	1.38E+01	-0.69	16	6.09E-02	3.60E+04	1.69E-06	26	1.62E-01	-2.29E+02	-7.08E-04	36	2.64E-01	-6.12E+02	-4.32E-04
7	2.15E+01	2.93E+00	7.33	17	7.11E-02	-8.09E+04	-8.78E-07	27	1.73E-01	-2.68E+02	-6.45E-04	37	2.74E-01	-6.50E+02	-4.22E-04
8	6.42E+00	-7.99E+00	-0.80	18	8.12E-02	-2.42E+04	-3.36E-06	28	1.83E-01	-3.06E+02	-5.98E-04				
9	-3.30E-01	-1.61E+00	0.20	19	9.14E-02	1.24E+03	7.35E-05	29	1.93E-01	-3.44E+02	-5.61E-04				
10	-6.99E+00	-5.01E-01	13.95	20	1.02E-01	2.63E+04	3.86E-06	30	2.03E-01	-3.82E+02	-5.31E-04				

Table 5-Zernike Coefficient Comparison

6. CLOSING THE LOOP

Improvements require mass removal or structural stiffening. A strain energy analysis will illustrate regions of the structure requiring mass removal or an increase in stiffness. After modifying the structure the analysis is repeated to evaluate the improvements.

Figure 10 is a strain energy analysis of mode 1.

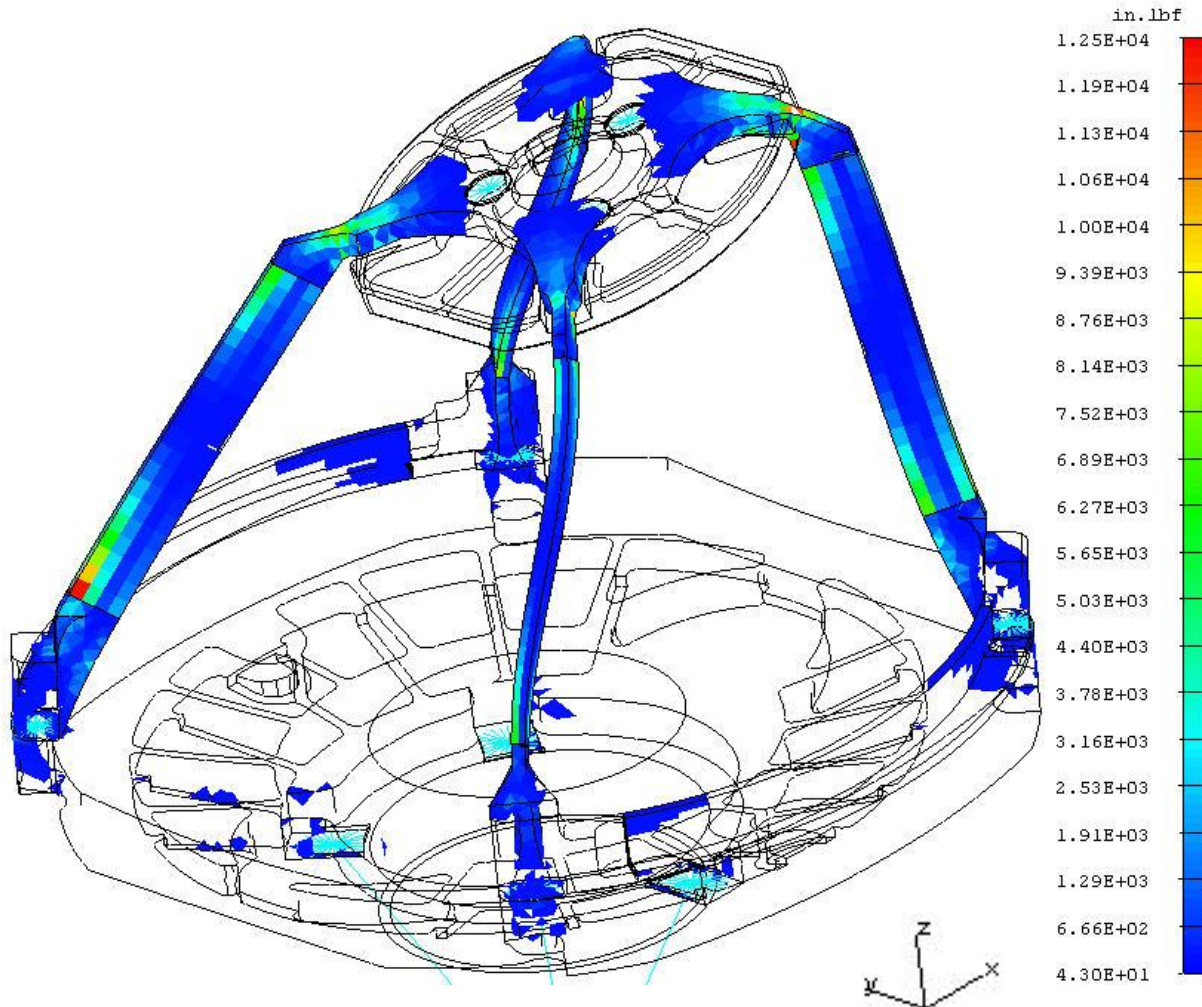


Figure 10

7. CONCLUSION

It has been shown how mechanical and optical analysis software can be used together to optimize an opto-mechanical structure subjected to vibrational loading. Mechanical analysis software output was post processed into Zernike polynomial coefficients and rigid body motions and analyzed with optical modeling software. Based on the results of these analyses, structural improvements can then be implemented where required.

For this example the static analysis results did not match the more rigorous random analysis results. A possible explanation is that the model's behavior did not match the assumptions required for the static analysis application.

The example analysis presented in this paper is intended to demonstrate the ability to design an opto-mechanical structure and optimize its performance without the cost and time associated with prototypes.

8. ACKNOWLEDGEMENTS

Dr. Victor Genberg, PhD and Greg Michels of Sigmadyne

9. REFERENCES

1. Steinberg, Dave S., *Vibration Analysis for Electronic Equipment, 3rd Edition*, John Wiley & Sons, Inc., New York, 2000